Inorganic Chemistry

Article

pubs.acs.org/IC

Syntheses, Structures, and Steady State and Time Resolved Photophysical Properties of a Tetraiminodiphenol Macrocyclic Ligand and Its Dinuclear Zinc(II)/Cadmium(II) Complexes with Coordinating and Noncoordinating Anions

Samit Majumder,* Leena Mandal, and Sasankasekhar Mohanta*

Department of Chemistry, University of Calcutta, 92 A. P. C. Road, Kolkata 700009, India

Supporting Information

ABSTRACT: The work in the present investigation reports the syntheses, structures, steady state, and time-resolved photophysical properties of a tetraiminodiphenol macrocyclic ligand H_2L and its eight dinuclear zinc(II) complexes and one cadmium(II) complex having composition $[Zn_2L(H_2O)_2](ClO_4)_2\cdot 2CH_3CN$ (**1**), $[Zn_2L(H_2O)_2](ClO_4)_2\cdot 2dmf$ (**2**), $[Zn_2L(H_2O)_2](NO_3)_2\cdot 2dmf$ (**3**), $[Zn_2LCl_2]$ (**4**), $[Zn_2L(N_3)_2]$ (**5**), $[Zn_2L(NCS)_2]$ (**6**), $[Zn_2L(NCO)_2]$ (**7**), $[Zn_2L(NCSe)_2]_2\cdot dmf$ (**8**), and $[Cd_2L(OAc)_2]$ (**9**) with various coordinating and noncoordinating anions. The structures of all the complexes **1**−**9** have been determined by single-crystal X-ray diffraction. The noncovalent interactions in the complexes result in the generation of the following topologies: two-dimensional network in **1**, **2**, **4**, **6**, **7**, **8**, and **9**; three-dimensional network in **5**. Spectrophotometric and spectrofluorometric titrations of the diprotonated salt $[H_4L](ClO_4)_2$ with triethylamine as well as with zinc(II) acetate and cadmium(II) acetate have been carried out, revealing fluorescence enhancement of the macrocyclic system by the base and the metal ions. Steady state fluorescence properties of $[H_4L](ClO_4)_2$ and **1**−**9** have been studied and their quantum yields have been determined. Time resolved fluorescence behavior of $[H_4L](ClO_4)_2$ and the dizinc(II) and dicadmium(II) complexes **1**−**9** have also been studied, and their lifetimes and radiative and nonradiative rate constants have been determined. The induced fluorescence enhancement of the macrocycle by zinc(II) and cadmium(II) is in line with the greater rate of increase of the radiative rate constants in comparison to the smaller rate of increase of nonradiative rate constants for the metal complexes. The fluorescence decay profiles of all the systems, being investigated here, that is, $[H_4L](ClO_4)_2$ and **1**−**9**, follow triexponential patterns, revealing that at least three conformers/components are responsible to exhibit the fluorescence decay behavior. The systems and studies in this report have been compared with those in the reports of the previously published similar systems, revealing some interesting aspects.

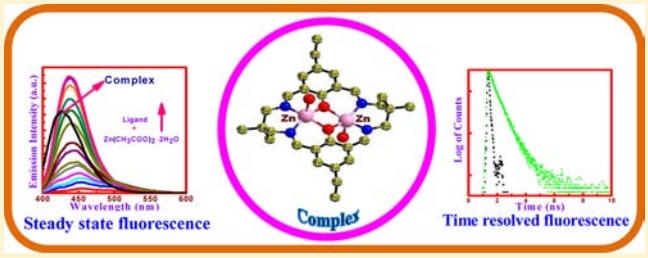

INTRODUCTION

Zinc is a ubiquitous and indispensable element[1,2] in the human body and the second most abundant metal ion after iron. Zinc is an essential cofactor[3] in six classes of enzymes as well as in several families of regulatory proteins. The active sites of the zinc containing metalloenzymes contain one, two, or three metal centers.[4] In addition to the biomimicking roles, some synthetic dinuclear[5] zinc(II) complexes are also known to participate in some biorelated processes. Because of the presence of the d^{10} electronic configuration, the common analytical techniques such as UV−Vis, Mössbauer, NMR, and EPR spectroscopy or magnetic susceptibility measurement can not be applied to detect zinc(II) ions in biological systems or in the systems in vitro. On the other hand, fortunately, emission spectroscopy of the zinc(II) complexes can be studied because zinc(II) can change the fluorescence intensity of organic fluorophores containing coordinating centers[6−12] and therefore fluorescence spectroscopy[9] has been the most powerful tool to detect this metal ion. Such fluorophores are thus zinc(II) sensors.[10−12] Similar to zinc(II), cadmium(II) has a spectroscopically silent d^{10} electronic configuration and in this case also fluorescence spectroscopy can be used as a detection tool for the same reason.[13] Therefore, search for reagents which can efficiently act as fluorescence sensors for zinc(II) and cadmium(II) has been an active area of research. There is another important orientation for the studies of the luminescence properties of zinc(II)/cadmium(II) complexes, namely, to explore the possibility of the systems to be used as electroluminescent materials for organic light emitting diodes.

Robson type tetraiminodiphenolate macrocyclic ligands obtained on condensation of 4-R-2,6-diformylphenol (R = methyl, chloro, butyl, trifluoromethyl, etc.)[14] and a diamine have been found as important Schiff base ligands in coordination chemistry research. Regarding zinc(II) or cadmium(II) complexes derived from this family of ligands,

Received: February 22, 2012
Published: August 7, 2012

dx.doi.org/10.1021/ic300412u | Inorg. Chem. 2012, 51, 8739−8749

although a number of zinc(II) complexes have been reported,[15] there is no example of a cadmium(II) complex. Again, photophysical properties of a small fraction of reported such zinc(II) complexes have been studied.[15a,b] Moreover, regarding the photophysical properties of such zinc(II) complexes and also of Robson type tetraiminodiphenolate macrocyclic ligands, only steady state properties have been investigated; there is no example of time-resolved fluorescence studies of such systems. This is in sharp contrast to the several reports on the photophysical properties of several zinc(II) and also cadmium(II) complexes in other type of ligand studies.[6,10−12,16,17] There are reports also of metal ion competition studies, competition between zinc(II) and other metal ion, with the purpose to understand the relative binding affinity and also to use the systems for fluorescence imaging or as fluorescence probe.[9,11,12] A few fluorescence probes of zinc(II) and cadmium(II) have been developed accordingly. However, the role of metal ions to effect the fluorescence properties of an organic fluorophore is highly system specific.[10−12] Therefore, as the fluorescence properties of Robson type macrocyclic ligands and their metal complexes are only little investigated, we have been motivated to explore this area with the expectation to get results which will be useful for developing structure−property correlations, which, in turn, may be useful to develop fluorescence probe, luminescent material, and imaging systems.

Recently, we have newly started studies of a system derived from ligands having 4-ethyl-2,6-diformylphenol as a fragment.[18] In comparison to the 4-methyl analogue, new and interesting structures/topologies/properties have already been observed in the complexes derived from an acyclic ligand having 4-ethyl-2,6-diformylphenol as a fragment.[18a] To explore further the systems having 4-ethyl-2,6-diformylphenol as a fragment and also to explore photophysical properties, of zinc(II)/cadmium(II) complexes derived from Robson type macrocyclic tetraiminodiphenolate ligands, we have synthesized eight dizinc(II) and one dicadmium(II) complexes derived from a macrocyclic ligand H_2L (Chart 1), which is the [2 + 2] condensation product of 4-ethyl-2,6-diformylphenol and 2,2′-dimethyl-1,3-diaminopropane. In these complexes we used several anions (perchlorate, nitrate, chloride, azide, cyanate, thiocyanate, and selenocyanate) with the expectation to monitor structure and properties as the function of coordinating and noncoordinating nature of the anions. Herein, we report syntheses, characterization, crystal and molecular structures, and steady state and time-resolved photophysical properties of these nine dinuclear complexes $[Zn_2L(H_2O)_2](ClO_4)_2\cdot 2CH_3CN$ (**1**), $[Zn_2L(H_2O)_2](ClO_4)_2\cdot 2dmf$ (**2**), $[Zn_2L(H_2O)_2](NO_3)_2\cdot 2dmf$ (**3**), $[Zn_2LCl_2]$ (**4**), $[Zn_2L(N_3)_2]$ (**5**), $[Zn_2L(NCS)_2]$ (**6**), $[Zn_2L(NCO)_2]$ (**7**), $[Zn_2L(NCSe)_2]_2\cdot dmf$ (**8**), and $[Cd_2L(OAc)_2]$ (**9**) and also of the diprotonated macrocyclic salt $[H_4L](ClO_4)_2$. We also report the spectrophotometric and spectrofluorometric titrations of $[H_4L](ClO_4)_2$ by a base, Et_3N, and by zinc(II) and cadmium(II) acetates as well as the fluorescence titration of $[H_4L](ClO_4)_2$ by various metal ions.

Chart 1. Chemical Structure of H_2L

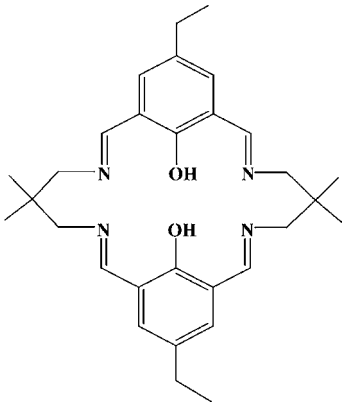

EXPERIMENTAL SECTION

Caution! *Perchlorate and azide complexes of metal ions are potentially explosive. Only a small amount of material should be prepared, and it should be handled with caution.*

Materials and Physical Methods. All reagents and solvents were purchased from commercial sources and used as received. 4-Ethyl-2,6-diformylphenol was synthesized by a known procedure.[19] $[H_4L](ClO_4)_2$ was synthesized by the reported method.[15a,b,18b] Elemental (C, H, and N) analyses were performed on a Perkin-Elmer 2400 II analyzer. IR spectra were recorded in the region 400−4000 cm^{-1} on a Bruker-Optics Alpha−T spectrophotometer with samples as KBr disks. The electrospray ionization mass spectra (ESI-MS positive) were recorded on a Micromass Qtof YA 263 mass spectrometer. Molar conductivity (Λ_M) of 1 mM solution in *N*,*N*-dimethylformamide (dmf) was measured at 298 K with a Systronics conductivity bridge. Absorbance spectra were obtained with a Shimadzu UV-3600/Hitachi U-3501 spectrophotometer, and a Perkin-Elmer LS-50B spectrofluorometer was utilized to study emission spectra. In all measurements, the sample concentration 2×10^{-5} M was maintained. Only freshly prepared solutions were used for the spectroscopic study, and all experiments have been carried out at room temperature (298 K). Time resolved fluorescence decay was recorded using a TCSPC lifetime system of Horiba Jobin Yvon IBH Ltd. having a picoseconds diode laser (Model: Fluorocube-01-NL).

Fluorescence quantum yields (φ) of the compounds were estimated at room temperature for their dmf solution by a relative method using anthracene[20a−g] (for **1**−**9**, φ = 0.36 in cyclohexane) and riboflavin[20h] (for the ligand, φ = 0.30 in ethanol) as the secondary standard using the following equation

$$\frac{\varphi_S}{\varphi_R} = \frac{I_S}{I_R} \times \frac{(OD)_R}{(OD)_S} \times \frac{\eta_S^2}{\eta_R^2}$$

Where I is the area under the emission spectral curve, OD denote absorbance at the wavelength of exciting light, η is the refractive index of the medium, φ is the fluorescence quantum yield, and the subscripts S and R stand in the recognition of the respective parameters of studied sample and reference, respectively.

Fluorescence lifetimes were determined from time-resolved intensity decay by the method of time correlated single-photon counting using a diode laser at 440 and 375 nm as light source. The excellence of the fits was judged by the χ^2 criterion. Average fluorescence lifetime ($\langle\tau_f\rangle$) for the multiexponential decay curve was obtained from the decay time constants (τ) and pre-exponential factors (α) using the following equation[21]

$$\langle\tau_f\rangle = \frac{\sum_i \alpha_i \tau_i^2}{\sum_i \alpha_i \tau_i}$$

in which α_i is the pre-exponential factor corresponding to the i-th decay time constant τ_i.

Synthesis. All these compounds were prepared in direct route on using $[H_4L](ClO_4)_2$ as the precursor for the organic ligand or in template route on using 4-ethyl-2,6-diformylphenol and 2,2′-dimethyl-1,3-diaminopropane as the precursors for the organic ligand. The metal salts used are as follows: $Zn(ClO_4)_2\cdot 6H_2O$ for **1** and **2**, either $Zn(ClO_4)_2\cdot 6H_2O$ and $NaNO_3$ or $Zn(NO_3)_2\cdot 6H_2O$ for **3**, either $Zn(ClO_4)_2\cdot 6H_2O$ and NaCl or $ZnCl_2$ for **4**, $Zn(ClO_4)_2\cdot 6H_2O$ and

dx.doi.org/10.1021/ic300412u | Inorg. Chem. 2012, 51, 8739−8749

Table 1. Crystallographic Data for 1−9

	1	2	3	4	5	6	7	8	9
empirical formula	$C_{34}H_{44}N_6Cl_2O_{12}Zn_2$	$C_{36}H_{50}N_6O_{14}Cl_2Zn_2$	$C_{36}H_{52}N_8O_{12}Zn_2$	$C_{30}H_{38}N_4O_2Cl_2Zn_2$	$C_{30}H_{38}N_{10}O_2Zn_2$	$C_{32}H_{38}N_6O_2S_2Zn_2$	$C_{32}H_{38}N_6O_4Zn_2$	$C_{35}H_{45}N_7O_3Se_2Zn_2$	$C_{34}H_{44}N_4O_6Cd_2$
formula weight	930.45	992.52	919.64	688.35	701.48	733.61	701.48	900.50	829.57
crystal system	orthorhombic	orthorhombic	orthorhombic	monoclinic	monoclinic	monoclinic	monoclinic	triclinic	triclinic
space group	*Pbcn*	*Pbcn*	*Pbcn*	*P*2(1)/*c*	*P*2(1)/*n*	*P*2(1)/*n*	$P2_1/c$	$P\bar{1}$	$P\bar{1}$
a (Å)	12.2766(15)	12.4183(16)	12.2586(10)	10.0033(7)	9.323(3)	18.486(2)	12.711(4)	9.7122(14)	8.9664(4)
b (Å)	19.514(3)	19.863(3)	19.7101(16)	12.2384(8)	9.027(3)	11.5384(13)	16.421(5)	12.8555(18)	9.0191(4)
c (Å)	18.050(2)	18.096(2)	17.9933(14)	13.0030(9)	19.506(7)	18.538(2)	19.282(5)	16.278(2)	12.6124(5)
α (deg)	90.00	90.00	90.00	90.00	90.00	90.00	90.00	83.847(4)	70.242(2)
β (deg)	90.00	90.00	90.00	107.016(3)	91.625(4)	117.6380(10)	128.227(14)	77.848(5)	86.565(2)
γ (deg)	90.00	90.00	90.00	90.00	90.00	90.00	90.00	84.073(4)	66.566(2)
V (Å^3)	4324.2(9)	4463.8(10)	4347.5(6)	1522.20(18)	1641.0(10)	3503.0(7)	3161.6(16)	1968.6(5)	877.44(7)
Z	4	4	4	2	2	4	4	2	1
D (calculated, g cm^{-3})	1.429	1.477	1.405	1.502	1.420	1.391	1.474	1.519	1.570
λ (Mo K$_\alpha$), Å	0.71073	0.71073	0.71073	0.71073	0.71073	0.71073	0.71073	0.71073	0.71073
μ (mm^{-1})	1.295	1.263	1.170	1.785	1.505	1.525	1.564	3.109	1.260
T (K)	296(2)	296(2)	296(2)	296(2)	296(2)	296(2)	296(2)	296(2)	296(2)
F(000)	1920	2056	1920	712	728	1520	1456	912	420
2θ range for data collection (deg)	3.92 − 50.46	3.86 − 51.04	3.92 − 50.66	4.26 − 54.00	4.18 − 52.00	2.58 − 50.14	3.66 − 47.18	2.56 − 51.90	3.44 − 56.62
index ranges	$-14 \le h \le 14$	$-15 \le h \le 15$	$-13 \le h \le 14$	$-12 \le h \le 12$	$-11 \le h \le 11$	$-21 \le h \le 22$	$-14 \le h \le 14$	$-11 \le h \le 10$	$-11 \le h \le 11$
	$-23 \le k \le 23$	$-24 \le k \le 22$	$-23 \le k \le 23$	$-15 \le k \le 15$	$-11 \le k \le 11$	$-13 \le k \le 13$	$-18 \le k \le 16$	$-15 \le k \le 15$	$-12 \le k \le 11$
	$-21 \le l \le 21$	$-21 \le l \le 21$	$-21 \le l \le 21$	$-15 \le l \le 15$	$-24 \le l \le 23$	$-22 \le l \le 21$	$-21 \le l \le 21$	$-20 \le l \le 20$	$-16 \le l \le 14$
no. measured reflections	29248	31079	48728	10041	11907	24684	19313	24287	10411
no. independent reflections	3901	4154	3974	3233	3195	6187	4722	7581	4262
R_{int}	0.0365	0.0501	0.0552	0.0338	0.0244	0.1044	0.0464	0.0352	0.0332
no. refined parameters	257	276	285	184	202	413	403	450	212
no. observed reflections, $I \ge 2\sigma(I)$	2952	2765	2840	2738	2646	2765	3710	5624	3724
goodness-of-fit on F^2, S	1.120	1.179	1.199	1.009	1.078	0.998	1.036	1.030	1.101
R_1[a], wR_2[b] [$I \ge 2\sigma(I)$]	0.0419, 0.1349	0.0652, 0.1749	0.0529, 0.1582	0.0326, 0.0732	0.0387, 0.1303	0.0504, 0.0653	0.0321, 0.0821	0.0419, 0.1325	0.0307, 0.0817
R_1[a], wR_2[b] [all data]	0.0589, 0.1512	0.0998, 0.1967	0.0789, 0.1844	0.0406, 0.0770	0.0485, 0.1397	0.1551, 0.0868	0.0480, 0.0912	0.0625, 0.1485	0.0387, 0.1072
max., min electron density (e Å^{-3})	0.646, −0.428	0.791, −0.946	0.517, −0.369	0.452, −0.839	0.828, −0.440	0.344, −0.320	0.270, −0.409	0.735, −0.894	0.763, −0.491

[a] $R_1 = [\sum||F_o| - |F_c||/\sum|F_o|]$. [b] $wR_2 = [\sum w(F_o^2 - F_c^2)^2/\sum w(F_o^2)^2]^{1/2}$.

dx.doi.org/10.1021/ic300412u | Inorg. Chem. 2012, 51, 8739−8749

NaN_3 for **5**, $Zn(ClO_4)_2·6H_2O$ and NH_4NCS for **6**, $Zn(ClO_4)_2·6H_2O$ and NaOCN for **7**, $Zn(ClO_4)_2·6H_2O$ and KSeCN for **8**, $Cd(OAc)_2·2H_2O$ for **9**. Acetonitrile was used as solvent for **1** and **9**, whereas dmf was used as solvent for **2**−**8**. As representative examples, syntheses of compounds **1** and **9** were described below following both direct and template routes.

Direct Route Synthesis of $[Zn_2L(H_2O)_2](ClO_4)_2·2CH_3CN$ (1). An acetonitrile solution (10 mL) of $Zn(ClO_4)_2·6H_2O$ (0.72 g, 2 mmol) was added to a stirred acetonitrile solution (15 mL) of $[H_4L](ClO_4)_2$ (0.689 g, 1 mmol). To the resulting reddish yellow solution was dropwise added an acetonitrile solution (5 mL) of triethylamine (0.404 g, 4 mmol) to get a yellow solution. After 2 h stirring, the yellow solution was filtered to eliminate out any suspended particles. The filtrate was kept at room temperature for slow evaporation. After a few days, a yellow crystalline compound containing diffraction quality single crystals that deposited was collected by filtration, washed with methanol, and air-dried. Yield: 0.79 g (85%). Anal. Calcd for (%) $C_{34}H_{48}N_6O_{12}Cl_2Zn_2$: C, 43.70; H, 5.18; N, 8.99. Found: C, 43.67; H, 5.24; N, 8.86. IR (KBr pellet, cm^{-1}): $\nu(H_2O)$, 3385(b); $\nu(C{=}N)$, 1641(s); $\nu(ClO_4)$, 1097(vs), 623(w).

Template Route Synthesis of $[Zn_2L(H_2O)_2](ClO_4)_2·2CH_3CN$ (1). To a boiling acetonitrile solution (20 mL) of 4-ethyl-2,6-diformylphenol (0.356 g, 2 mmol) and $Zn(ClO_4)_2·6H_2O$ (0.72 g, 2 mmol) was added a methanol solution (20 mL) of 2,2′-dimethyl-1,3-diaminopropane (0.204 g, 2 mmol). The resulting deep yellow solution was refluxed for 2 h and after cooling the yellow solution was filtered to eliminate out any suspended particles. The filtrate was kept at room temperature for slow evaporation. After a few days, yellow crystalline compound containing diffraction quality single crystals that deposited was collected by filtration, washed with methanol, and air-dried. Yield: 0.77 g (83%). Analytical data are almost identical with those mentioned above. FT-IR spectrum is superimposable with that of the compound obtained by direct route synthesis.

Direct Route Synthesis of $[Cd_2L(OAc)_2]$ (9). An acetonitrile solution (10 mL) of cadmium(II) acetate dihydrate (0.533 g, 2 mmol) was added to a stirred acetonitrile solution (15 mL) of $[H_4L](ClO_4)_2$ (0.689 g, 1 mmol). After 2 h stirring, the yellow solution was filtered to eliminate out any suspended particles. The filtrate was kept at room temperature for slow evaporation. After a few days, a yellow crystalline compound containing diffraction quality single crystals that deposited was collected by filtration, washed with methanol, and air-dried. Yield: 0.58 g (70%). Anal. Calcd for (%) $C_{34}H_{44}N_4O_6Cd_2$: C, 49.23; H, 5.35; N, 6.75. Found: C, 49.25; H, 5.34; N, 6.77. IR (KBr pellet, cm^{-1}): $\nu(C{=}N)$, 1642(s); $\nu(CH_3COO)$, 1546(vs), 1430(s).

Template Route Synthesis of $[Cd_2L(OAc)_2]$ (9). To a boiling acetonitrile solution (10 mL) of 4-ethyl-2,6-diformylphenol (0.356 g, 2 mmol) were added successively an acetonitrile solution (10 mL) of cadmium(II) acetate dihydrate (0.533 g, 2 mmol) and an acetonitrile solution (10 mL) of 2,2′-dimethyl-1,3-diaminopropane (0.204 g, 2 mmol). The resulting deep yellow solution was refluxed for 1 h and then was filtered to eliminate out any suspended particles. The filtrate was kept at room temperature for slow evaporation. After a few days, yellow crystalline compound containing diffraction quality single crystals that deposited was collected by filtration, washed with methanol, and air-dried. Yield: 0.55 g (66%). Analytical data are almost identical with those mentioned above. The FT-IR spectrum is superimposable with that of the compound obtained by direct route synthesis.

Data for ***2***. Yield: 0.80 g (80%). Anal. Calcd for (%) $C_{36}H_{56}N_6O_{14}Cl_2Zn_2$: C, 43.30; H, 5.65; N, 8.42. Found: C, 43.28; H, 5.67; N, 8.39. IR (KBr pellet, cm^{-1}): $\nu(H_2O)$, 3383(b); $\nu(C{=}N)$, 1642(s); $\nu(ClO_4)$, 1097(vs), 623(w).

Data for ***3***. Yield: 0.69 g (75%). Anal. Calcd for (%) $C_{36}H_{56}N_8O_{12}Zn_2$: C, 46.81; H, 6.11; N, 12.13. Found: C, 46.79; H, 6.13; N, 12.12. IR (KBr pellet, cm^{-1}): $\nu(H_2O)$, 3449(b); $\nu(C{=}N)$, 1638(s); $\nu(NO_3)$, 1436 (s), 1384(s).

Data for ***4***. Yield: 0.48 g (70%). Anal. Calcd for (%) $C_{30}H_{38}N_4O_2Cl_2Zn_2$: C, 52.35; H, 5.56; N, 8.14. Found: C, 52.34; H, 5.54; N, 8.15. IR (KBr pellet, cm^{-1}): $\nu(C{=}N)$ 1632(s).

Data for ***5***. Yield: 0.56 g (80%). Anal. Calcd for (%) $C_{30}H_{38}N_{10}O_2Zn_2$: C, 51.37; H, 5.46; N, 19.97. Found: C, 51.39; H, 5.49; N, 19.95. IR (KBr pellet, cm^{-1}): $\nu(N_3)$, 2057(s); $\nu(C{=}N)$, 1636(s).

Data for ***6***. Yield: 0.55 g (75%). Anal. Calcd for (%) $C_{32}H_{38}N_6O_2S_2Zn_2$: C, 52.39; H, 5.22; N, 11.46. Found: C, 52.41; H, 5.23; N, 11.43. IR (KBr pellet, cm^{-1}): $\nu(SCN)$, 2080(vs); $\nu(C{=}N)$, 1638(s).

Data for ***7***. Yield: 0.53 g (75%). Anal. Calcd for (%) $C_{32}H_{38}N_6O_4Zn_2$: C, 54.79; H, 5.46; N, 11.98. Found: C, 54.81; H, 5.45; N, 11.96. IR (KBr pellet, cm^{-1}): $\nu(OCN)$, 2232(s); $\nu(C{=}N)$, 1637(s).

Data for ***8***. Yield: 0.65 g (75%). Anal. Calcd for (%) $C_{67}H_{83}N_{13}O_5Se_4Zn_4$: C, 46.57; H, 4.84; N, 10.54. Found: C, 46.51; H, 4.76; N, 10.62. IR (KBr pellet, cm^{-1}): $\nu(SeCN)$, 2082(s); $\nu(C{=}N)$, 1640(s).

Crystal Structure Determination of 1−9. The crystallographic data of all the compounds **1**−**9** are summarized in Table 1. Diffraction data of **1**−**9** were collected at 296 K on a Bruker-APEX II SMART CCD diffractometer using graphite-monochromated Mo−Kα radiation (λ = 0.71073 Å). The packages SAINT[22a] and SADABS[22b] were used for data processing and absorption correction. The structures were solved by direct and Fourier methods and refined by full-matrix least-squares based on F^2 using SHELXTL[22c] and SHELXL-97[22d] packages. During the development of the structures of **3** and **6**, it became apparent that two nitrate oxygen atoms O4 and O6 and one ethyl carbon atom C8 were disordered. These atoms were modeled with the occupancies 0.5/0.5 for O4, 0.8/0.2 for O6, and 0.5/0.5 for C8. It was not possible to locate all the four hydrogens of the two coordinated water molecules in **1**−**3**. The hydrogen atom linked with the amide carbon (C18) of the dmf molecule in **2** could not be inserted. All the remaining hydrogen atoms were placed at fixed geometrical position and refined freely. The hydrogen atoms were refined isotropically, while the nonhydrogen atoms were refined anisotropically. The final refinements converged at the R_1 values ($I > 2\sigma(I)$) 0.0419, 0.0652, 0.0529, 0.0326, 0.0387, 0.0504, 0.0321, 0.0419, and 0.0307for **1**−**9**, respectively.

RESULTS AND DISCUSSION

Synthesis and Characterization. The syntheses of the complexes are demonstrated in Supporting Information, Scheme S1. All the compounds are readily synthesized following direct route or template route. The perchlorate compound (**2**) having dmf as solvent of crystallization and the chloro, azide, thiocyanate, cyanate, and selenocyanate complexes (**4**−**8**) could also be prepared using the perchlorate compound (**1**) having acetonitrile as solvent of crystallization as the starting material.

The FT-IR spectra reveal the presence of C═N moieties in $[H_4L](ClO_4)_2$ (1666 cm^{-1}) and **1**−**9** (1632−1642 cm^{-1}), perclorate in $[H_4L](ClO_4)_2$ (1088 and 625 cm^{-1}) and **1**/**2** (1097 and 623 cm^{-1}), nitrate in **3** (1436 and 1384 cm^{-1}), acetate in **9** (1546 and 1430 cm^{-1}) azide in **5** (2057 cm^{-1}), thiocyanate in **6** (2080 cm^{-1}), cyanate in **7** (2232 cm^{-1}), selenocyanate in **8** (2082 cm^{-1}), and water molecules in **1**−**3** (3383−3449 cm^{-1}).

The molar conductance values of the complexes **1**−**9** were measured in dmf. The 2:1 electrolytic nature of the complexes **1**−**3** and the nonelectrolytic nature of **4**, **5**, **7**, and **9** in the solid state are retained in solution as evidenced by their molar conductance values[23] (134−171 ohm^{-1} cm^{-1} mol^{-1} L for **1**−**3**, 4.5−21 ohm^{-1} cm^{-1} mol^{-1} L for **4**, **5**, **7**, and **9**). In contrast, conductance values of **6** (76 ohm^{-1} cm^{-1} mol^{-1} L) and **8** (147 ohm^{-1} cm^{-1} mol^{-1} L) indicate that the composition of the complex species is 1:1 (**6**) and 2:1 (**8**) in solution, that is, different from those in the solid state.

dx.doi.org/10.1021/ic300412u | Inorg. Chem. 2012, 51, 8739−8749

Composition of the complexes **1**−**3** were further verified by electrospray ionization mass spectra (ESI−MS positive) in acetonitrile (ESI-MS spectra of other six compounds were not recorded because they are practically insoluble in common solvents except in dmf). Both the complexes $[Zn_2L(H_2O)_2](ClO_4)_2\cdot 2dmf$ (**2**; Supporting Information, Figure S1) and $[Zn_2L(H_2O)_2](NO_3)_2\cdot 2dmf$ (**3**; Supporting Information, Figure S2) exhibit two abundant peaks at m/z 644 (67% for **2** and 37% for **3**; line to line separation 1.0) and 309 (100% for **2** and **3**; line to line separation 0.5), while only the m/z = 309 peak (100%, line to line separation 0.5) is observed in the spectrum of $[Zn_2L(H_2O)_2](ClO_4)_2\cdot 2CH_3CN$ (**1**; Supporting Information, Figure S3). The peaks at m/z 309 and 644 are assignable to a dicationic $[Zn_2(L)]^{2+}$ ($C_{30}H_{38}N_4O_2Zn_2$) and a mononuclear monocationic species $[Zn(LH)(H_2O)(dmf)]^+$ ($C_{33}H_{49}N_5O_4Zn$) species. As shown in Supporting Information, Figures S1, S2, and S3, the isotopic distribution of the observed and simulated spectral patterns are in excellent agreement with each other, indicating right assignment.

Description of Structures of the Complexes 1−9. Crystal structures of complexes $[Zn_2L(H_2O)_2](ClO_4)_2\cdot 2CH_3CN$ (**1**) and $[Cd_2L(OAc)_2]$ (**9**) are shown in Figures 1 and 2, respectively, while the crystal structures of

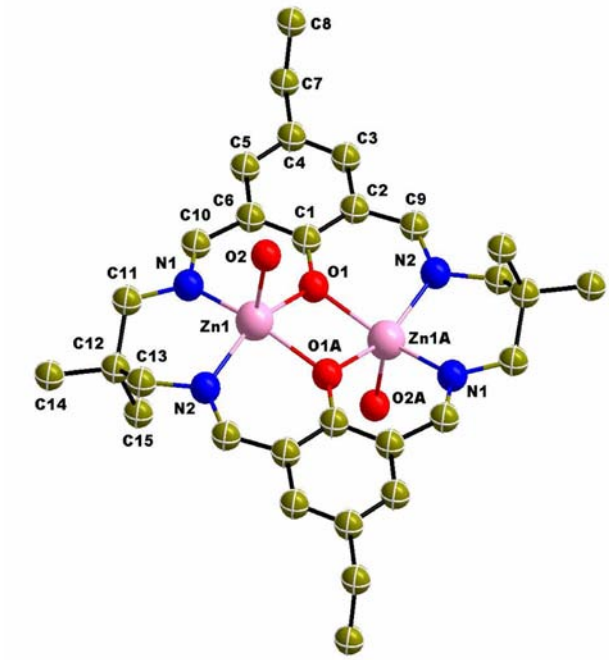

Figure 1. Crystal structure of $[Zn_2L(H_2O)_2](ClO_4)_2\cdot 2CH_3CN$ (**1**). Hydrogen atoms, perchlorate anions, and acetonitrile molecules are omitted for clarity. Symmetry code: A, 2−x, 1−y, 2−z.

$[Zn_2L(H_2O)_2](ClO_4)_2\cdot 2dmf$ (**2**), $[Zn_2L(H_2O)_2](NO_3)_2\cdot 2dmf$ (**3**), $[Zn_2LCl_2]$ (**4**), $[Zn_2L(N_3)_2]$ (**5**), $[Zn_2L(NCS)_2]$ (**6**), $[Zn_2L(NCO)_2]$ (**7**), and $[Zn_2L(NCSe)_2]_2\cdot dmf$ (**8**) are shown in Supporting Information, Figures S4−S10, respectively. Selected bond lengths and angles of **1**−**9** are listed in Supporting Information, Tables S1−S9. The structures show that the nine compounds are diphenoxo-bridged Zn^{II}_2 (**1**−**8**) or Cd^{II}_2 (**9**) systems derived from the tetraimino diphenolate macrocyclic ligand $[L]^{2-}$. The diphenoxo-bridged dinuclear moiety is dipositive cationic in the complexes **1**, **2**, and **3**, where the charge is balanced by two perchlorates (in **1** and **2**) or

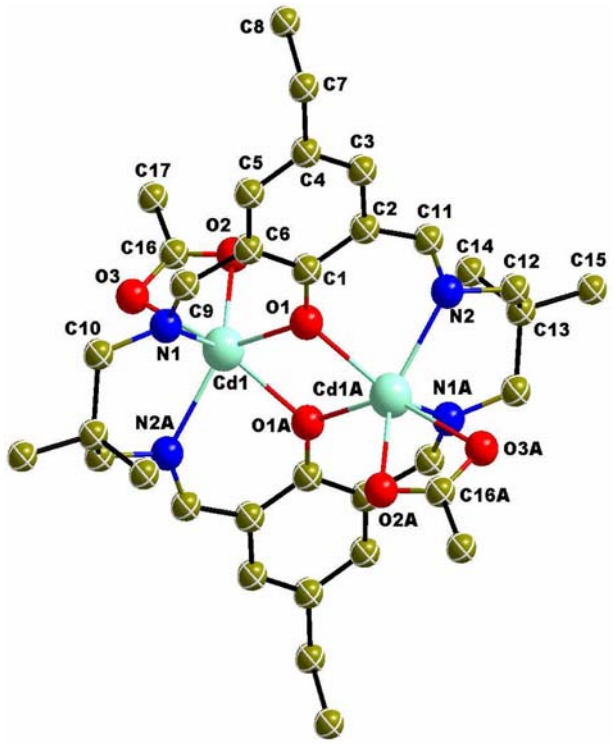

Figure 2. Crystal structure of $[Cd_2L(OAc)_2]$ (**9**). Hydrogen atoms are omitted for clarity. Symmetry code: A, 2−x, 1−y, 1−z.

nitrates (in **3**). In other six complexes, the diphenoxo-bridged dinuclear moiety is neutral in which each of the two metal ions are coordinated to each of the two anionic ligands, monodentate (chloride in **4**, azide in **5**, thiocyanate in **6**, cyanate in **7**, selenocyanate in **8**) or bidentate chelating (acetate in **9**). For **8**, there are two independent dinuclear units, which are almost identical.

Each of the two $N(imine)_2O(phenolate)_2$ compartments are coordinated to each of the two metal ions in all these complexes. In all the dizinc(II) complexes **1**−**8**, zinc(II) centers are pentacoordinated and adopt slightly distorted square pyramidal geometry in which the two imine nitrogen and two phenoxo oxygen atoms form the basal plane. The slightly distorted square pyramidal environment in each case is evidenced by the discrimination parameter (τ) value, in between 0.0003−0.1323. In the case of the dicadmium(II) compound **9**, the hexacoordinated CdN_2O_4 environment can not be modeled with any regular or distorted geometry because acetate chelates to a metal center from one side of the N_2O_2 ligand compartment. The metal centers in all of **1**−**9** displace significantly (0.4152−0.5989 Å in **1**−**8**, 0.9301 Å in **9**) toward the apical atoms in **1**−**8** or toward the acetate ligand in **9**.

The Zn−N(imine) and Zn−O(phenoxo) bond distances for all the complexes lie in the range 2.038(3)−2.120(3) Å and 2.040(2)−2.092(2) Å, respectively. The two Cd−O(phenoxo) bond distances are not very different, 2.257(2) Å and 2.276(2) Å, as are the two Cd−N(imine) bond distances, 2.285(3) Å and 2.292(3) Å. The dihedral angle values (0° in **1**−**5**, **8**, and **9**, 10.7° in **6**, 9.5° in **7**) between the two phenyl rings indicate that the whole molecule in **1**−**9** may be considered as more or less planar. The distance between two metal centers and the Zn−O(phenoxo)−Zn bridging angle for all the complexes **1**−**8** lie in the range between 3.227−3.285 Å and 103.23(9)−105.87(9)°, respectively. The Cd···Cd separation and Cd−

dx.doi.org/10.1021/ic300412u | Inorg. Chem. 2012, 51, 8739−8749

O(phenoxo)−Cd bridge angle are 3.611 Å and 105.61(9)°, respectively.

The individual dinuclear units in **1**, **2**, and **4**−**9** are self-assembled because of hydrogen bonding interactions to generate two-dimensional (in **1**, **2**, **4**, **6**−**9**) or three-dimensional (in **5**) topology. Description and demonstration (Supporting Information, Figures S11−S20) of the self-assemblies and the geometries of the hydrogen bonds (Supporting Information, Table S10) are given in Supporting Information.

Effect of Base on Absorption and Emission Spectra of $H_4L(ClO_4)_2$. Because of the presence of acidic N^+−H group in the ligand backbone, the spectral characteristics of the macrocyclic ligand can be influenced by base. Both the spectrophotometric and spectrofluorimetric titrations have been carried out to understand the effect of base such as triethylamine on $[H_4L](ClO_4)_2$. Figures 3 and 4 show the

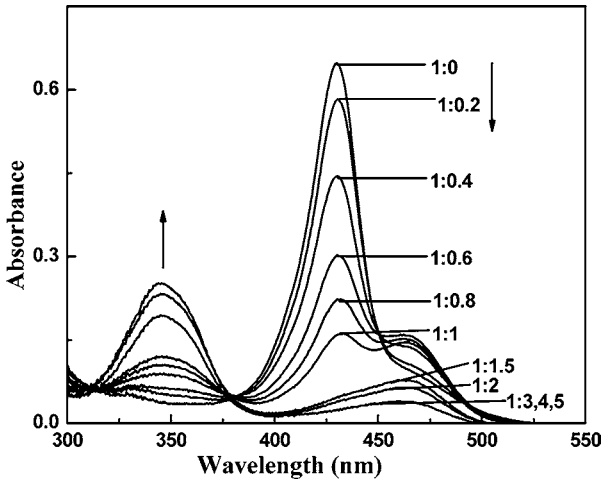

Figure 3. Spectrophotometric titration of diprotonated macrocyclic salt $[H_4L](ClO_4)_2$ (2×10^{-5} M) with triethylamine (2×10^{-5} M) in acetonitrile. Equivalent ratio of the macrocyclic system and triethylamine have been indicated in the figure.

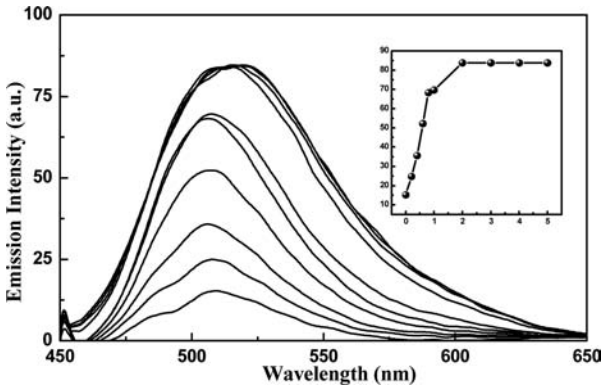

Figure 4. Changes in emission intensity of the diprotonated macrocyclic salt $[H_4L](ClO_4)_2$ (2×10^{-5} M) in acetonitrile upon addition of triethylamine (2×10^{-5} M). The inset shows the variation of the emission intensity with number of equivalents of triethylamine added. λ_{ex} = 432 nm.

changes in absorption and emission profiles, respectively, of the ligand in acetonitrile with the incremental addition of triethylamine. It is evident from Figure 3 that $[H_4L](ClO_4)_2$ exhibits one band at 432 nm and one shoulder at 464 nm. While the band at 432 nm arises because of $\pi \rightarrow \pi^*$ transitions of the azomethine moiety,[15b,24] the band at 464 nm could be simply a vibronic transition. During the first 1 equivalent base addition, the following changes take place: (ii) the intensity of the band at 464 nm is increased; (i) the intensity of the band at 432 nm is decreased; (iii) A new band at 345 nm appeared. On adding more amount of base, the intensity of both the bands at 464 and 432 nm is reduced and the intensity of the new band at 345 nm is enhanced gradually until a saturation occurs at 1:3 of $[H_4L](ClO_4)_2/Et_3N$ ratio when the original bands of $[H_4L](ClO_4)_2$ disappeared. All the absorption curves in this spectrophotometric titration pass through an isosbestic point at about 380 nm, clearly indicating that the deprotonation process takes place more or less smoothly, and there exists an equilibrium in the deprotonation process. It may be mentioned that $\pi \rightarrow \pi^*$ transition of the azomethine moiety is shifted significantly from 432 nm in $[H_4L](ClO_4)_2$ to 345 nm in the mixture of $[H_4L](ClO_4)_2$ and Et_3N simply because of the significant change of the chromophore; while the imine nitrogen atoms are protonated, deprotonation takes place in the mixture. Such shifting was observed in other examples.[15b,24]

As shown in the Figure 4, the fluorescence intensity increases with gradual increase of the amount of base without any change in its position until ligand to base ratio 1:1 (emission occurs at 507 nm) is reached. Further addition of base up to 1:3 ratio of ligand to base results in gradual increase of fluorescence intensity with red-shifting of the emission maxima by 7 nm (emission occurs at 514 nm). The spectral pattern remains unchanged on adding more amount of base.

Spectrophotometric and Spectrofluorimetric Titration of $H_4L(ClO_4)_2$ with $Zn(OAc)_2 \cdot 2H_2O$ and $Cd(OAc)_2 \cdot 2H_2O$ and the Fluorescence Spectra of 1−9. The reaction equilibria involving the macrocyclic ligand system $H_4L(ClO_4)_2$ and $Zn(OAc)_2 \cdot 2H_2O/Cd(OAc)_2 \cdot 2H_2O$ in acetonitrile have been followed spectrophotometrically (Figure 5 and Supporting Information, Figure S21, respectively) as well as spectrofluorimetrically (Figure 6 and Supporting Information, Figure S22, respectively) by observing the spectral changes upon incremental addition of the metal acetate until no further change is noted. The absorption and emission profiles for both

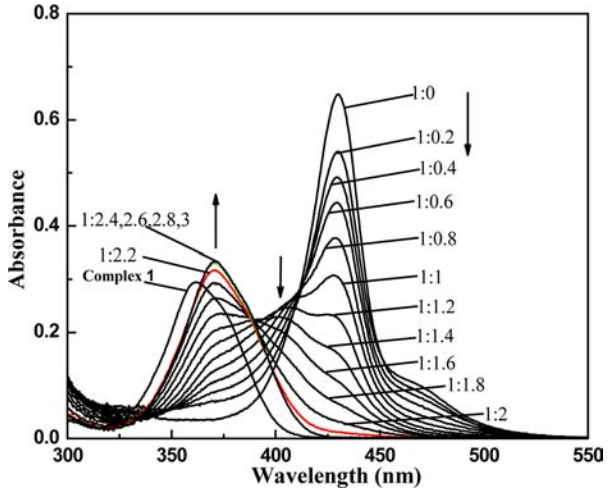

Figure 5. Spectrophotometric titration of the diprotonated macrocyclic salt $[H_4L](ClO_4)_2$ (2×10^{-5} M) with $Zn(OAc)_2 \cdot 2H_2O$ in acetonitrile. Equivalent ratio of the macrocyclic system and $Zn(OAc)_2 \cdot 2H_2O$ have been indicated in the figure.

dx.doi.org/10.1021/ic300412u | Inorg. Chem. 2012, 51, 8739−8749

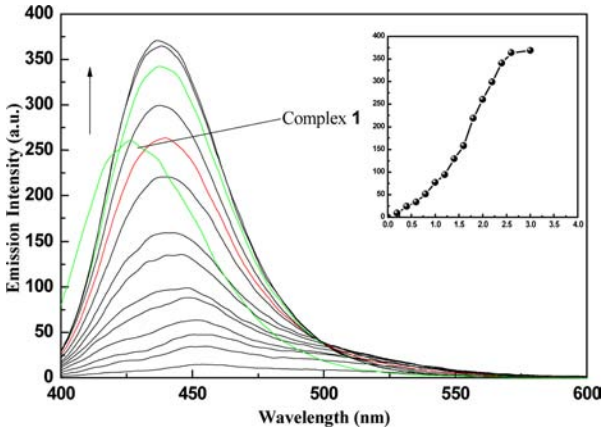

Figure 6. Spectrofluorimetric titration of the diprotonated macrocyclic salt $[H_4L](ClO_4)_2$ (2×10^{-5} M) with $Zn(OAc)_2 \cdot 2H_2O$ in acetonitrile. The arrow indicates the increasing concentration of $Zn(OAc)_2 \cdot 2H_2O$ added. The inset shows the variation of the emission intensity with number of equivalents of $Zn(OAc)_2 \cdot 2H_2O$ added. λ_{ex} = 370 nm.

the metal ions are similar indicating the mode of metal binding to the macrocyclic cavity is similar in nature.

It can be seen from Figure 5 and Supporting Information, Figure S21 that the intensity of both the bands of $[H_4L](ClO_4)_2$ at 464 and 432 nm is reduced during incremental addition of both the metal acetates. During the first 1 equivalent metal ion addition, a new band is generated at 405 and 409 nm for zinc(II) and cadmium(II), respectively. On adding more amount of acetate salts, the intensity of the band at 405/409 nm is reduced with the simultaneous generation of another new band at 370 nm for zinc(II) and 375 nm for cadmium(II). The saturation takes place at 2.4 equiv of zinc(II) and 2.6 equiv of cadmium(II). The saturated spectra consists of only one band at 370/375 nm. The dizinc(II) compounds **1**−**8** (in acetonitrile or dmf for **1**−**3** and dmf for **4**−**8**) and the dicadmium(II) compound **9** (in dmf) also exhibit one spectral band and, moreover, the peak position of the saturated spectra (in acetonitrile) for both the zinc(II) and cadmium(II) cases are almost identical with the band maxima of the corresponding dinuclear complexes (spectrum of one Zn^{II}_2 complex **1** is shown in Figure 5 and spectrum of the Cd^{II}_2 complex **9** is shown in Supporting Information, Figure S21). It may be mentioned that the band at 370 nm for the Zn^{II}_2 complexes and at 375 nm for the Cd^{II}_2 complex arise because of $\pi \rightarrow \pi^*$ transition. Clearly, as observed in previous cases,[12g,15a,b,16j] the ligand-centered azomethine $\pi \rightarrow \pi^*$ transition of $H_4L(ClO_4)_2$ is perturbed significantly (from 432 nm to 370/375 nm) by complexation with zinc(II) and cadmium(II).

The generation of the two bands at about 407 and 373 nm at the two stages of the spectrophotometric titrations indicates that the complex formation takes place in stepwise manner. In spite of the stepwise formation of the complex species, it was not possible to isolate the mononuclear zinc(II)/cadmium(II) complex. Evidently, two equilibrium constants are overlapped. All the absorption curves in the spectrophotometric titration by both zinc(II) and cadmium(II) acetate pass to an isosbestic point at about 389 nm, clearly indicating that the complexation take place more or less smoothly.

As shown in Figure 6 and Supporting Information, Figure S22, upon excitation at 370 and 375 nm (λ_{max} for the dizinc(II) complex and λ_{max} for the dicadmium(II) complex, respectively), the emission intensity gradually increases with the addition of both metal ions, and the emission maximum is gradually blue-shifted from 455 to 436 nm for zinc(II) and from 495 to 445 nm for cadmium(II). The saturation occurs at the $[H_4L](ClO_4)_2$/metal acetate ratio of 1:2 and 1:2.2 for zinc(II) and cadmium(II), respectively. On exciting at 370 nm for the zinc(II) complexes **1**−**8** (in acetonitrile or dmf for **1**−**3** and dmf for **4**−**8**) and at 375 nm for the cadmium(II) complex **9** (in dmf), the position of the emission spectra of the complexes is identical to that of the emission spectra of the corresponding saturated solutions during spectrofluorometric titration (one representative example for each case is shown in Figures 6 and Supporting Information, Figure S22).

The fluorescence spectra of **1**−**9** in dmf are compared in Figure 7. The fluorescence enhancement of the macrocyclic

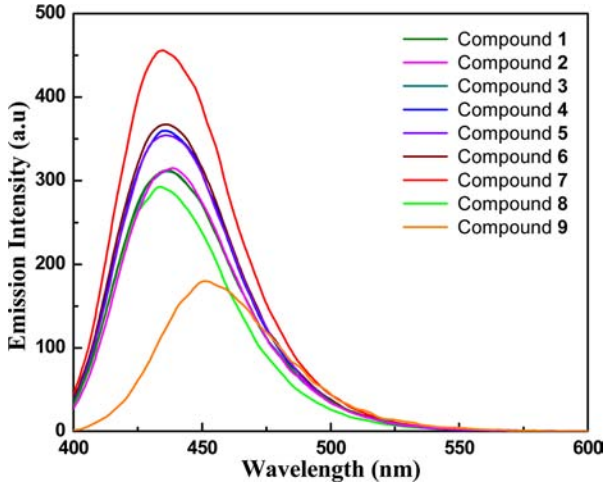

Figure 7. Fluorescence spectra of **1**−**9** in dmf (2×10^{-5} M).

moiety in presence of zinc(II) or cadmium(II) is supported from their calculated quantum yield values, Table 2. The incorporation of the metal ion into the ligand leads to the modulation of the photophysical response of the ligand. For the complexes, no emission originating from metal-centered MLCT/LMCT excited states are expected, since the Zn(II) and Cd(II) ion are difficult to oxidize or reduce because of their stable d^{10} electronic configuration. Thus, the emission observed in the complexes can be tentatively assigned to the $\pi \rightarrow \pi^*$ intraligand fluorescence. The incorporation of Zn(II) and Cd(II) effectively increases the conformational rigidity and thus enhance the fluorescence intensities as fluorescence behavior is closely associated with the metal ions and the ligand coordinated around them.

Time Resolved Fluorescence Studies. To gain more insight on the change of excited state decay process, the time correlated single photon counting (TCSPC) of $[H_4L](ClO_4)_2$ (Figure 8), the Zn^{II}_2 complexes **1**−**8** (Figure 9 for compound **1** and Supporting Information, Figure S23−S29 for compounds **2**−**8**), and the Cd^{II}_2 compound **9** (Supporting Information, Figure S30) was measured, from which lifetime and rate constants of both radiative and nonradiative decay processes were calculated. All the fluorescence decay profiles of $[H_4L](ClO_4)_2$ (at 512 nm), of the Zn^{II}_2 complexes **1**−**8** (at 436 nm), and of the Cd^{II}_2 compound **9** (at 445 nm) were best fitted with triexponential decay, indicating that at least three components/conformations are responsible for the fluorescence behavior of $[H_4L](ClO_4)_2$, **1**−**8** and **9**. Although it is very difficult and may even be misleading to get the exact clear

dx.doi.org/10.1021/ic300412u | Inorg. Chem. 2012, 51, 8739−8749

Table 2. Photoluminescent Data for the Ligand and 1−9 at Room Temperature

compound	λ_{ex}	λ_{em}	φ	τ (ns)[a]	K_r ($\times 10^{-6}$ s^{-1})	K_{nr} ($\times 10^{-8}$ s^{-1})	χ^2
$[H_4L](ClO_4)_2$	432	512	0.0025	1.0313	2.4	9.67	1.134
1	370	436	0.0115	0.5266	21.84	18.96	1.017
2	370	436	0.01148	0.6647	17.27	14.87	1.072
3	370	436	0.01677	0.6503	25.78	15.12	1.014
4	370	436	0.02576	0.4471	57.61	21.79	1.017
5	370	436	0.01577	0.5027	31.37	19.57	1.034
6	370	436	0.01603	0.6588	24.33	14.94	1.003
7	370	436	0.01709	0.5182	32.97	18.96	1.008
8	370	436	0.0048	0.5084	9.44	19.57	1.014
9	375	446	0.0075	0.71498	10.48	13.88	1.144

[a]Average.

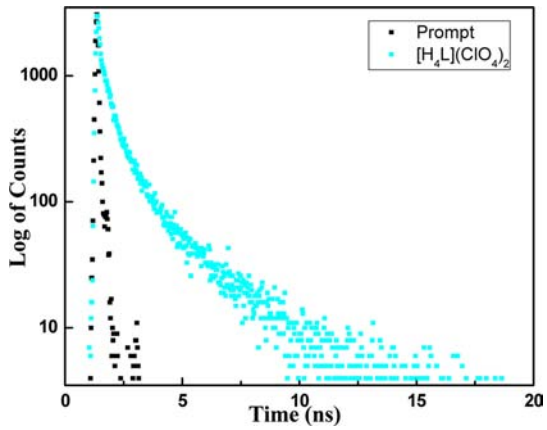

Figure 8. Time-resolved fluorescence decay of the diprotonated macrocyclic salt $[H_4L](ClO_4)_2$ in dmf. The fluorescence was monitored at 512 nm.

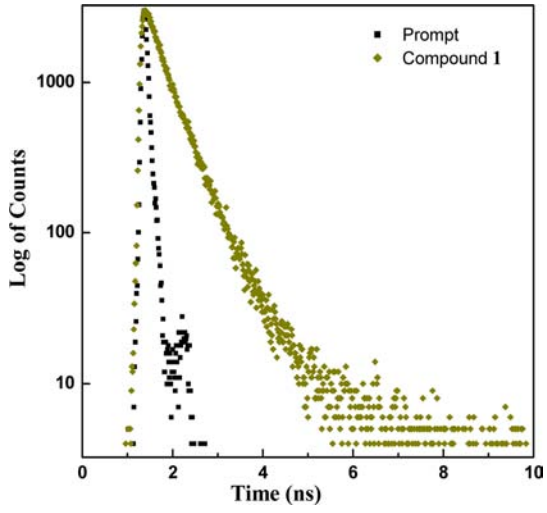

Figure 9. Time-resolved fluorescence decay of $[Zn_2L(H_2O)_2](ClO_4)_2{\cdot}2CH_3CN$ (**1**) in dmf. The fluorescence was monitored at 436 nm.

information about all the components/conformations responsible for fluorescence, the complicated behavior of $[H_4L](ClO_4)_2$ at least may be attributed to the possible existence of different hydrogen-bonded species of the macrocycle formed with the surrounding solvent DMF molecules.

As $[H_4L](ClO_4)_2$, **1**−**8**, and **9** follow triexponential decay, it is not possible to specify the particular values of the rate constants. Therefore, instead of giving emphasis on individual components, we preferred to use the mean fluorescence lifetime. The radiative rate constant (K_r) and the nonradiative rate constant (K_{nr}) of $[H_4L](ClO_4)_2$ and the complexes **1**−**9** were calculated and are listed in Table 2. It is evident from the list that both K_r and K_{nr} are increased for the complexes **1**−**9** in comparison to $[H_4L](ClO_4)_2$. But as the relative increase of K_r (∼4 times for **8** and **9** and ∼7−24 times for **1**−**7**) is much greater than that of K_{nr} (∼ 1.4−2.2 times for **1**−**9**), the induced fluorescence enhancement $[H_4L](ClO_4)_2$ by zinc(II) and cadmium(II) mainly can be ascribed to the increase of K_r. Actually, complexation would impose rigidity to the ligand and hence increase the value of radiative rate constant.

The K_{nr} and lifetime for the Zn^{II}_2 complexes **1**−**8** are not very different (Table 2). However, no correlation of K_{nr} with other parameters could be found. On the other hand, K_r and quantum yield for **1**−**8** follow an approximate relationship: the more the value of K_r, the more the value of the quantum yield.

As already discussed, the metal centers in the Zn^{II}_2 complexes **4**, **5**, **6**, **7**, and **8** are coordinated to anions, chloride, azide, thiocyanate, cyanate, and selenocyanate, respectively. It can be seen from Table 2 that both K_r and φ are largest (57.61×10^6 s^{-1} and 0.02576) for the chloro compound **4**, while these are smallest (9.44×10^6 s^{-1} and 0.0048) for the selenocyanate compound **8**. These values are intermediate for the azide, thiocyanate and isocyanate compounds **5** (31.37×10^6 s^{-1} and 0.01577), **6** (24.33×10^6 s^{-1} and 0.01603), and **7** (32.97×10^6 s^{-1} and 0.01709). It seems from this comparison that the fluorescence behavior is effected by the nature of coordinating anion. Although such effects on the fluorescence behavior of gold(I) systems are known, the dependency of fluorescence on coordinated anions[25] is a new observation in zinc(II) complexes.

Metal Ion Competition Studies. To investigate the fluorescent selectivity of the ligand for various transition metal ions in detail, the fluorescent spectra of acetonitrile solutions of $[H_4L](ClO_4)_2$, Et_3N and a metal perchlorate were studied systematically for a number of metal ions, Zn^{II}, Cu^{II}, Ni^{II}, Co^{II}, Fe^{II}, Mn^{II}, Cd^{II}, Hg^{II}. The concentrations of $[H_4L](ClO_4)_2$, Et_3N and metal perchlorate in the solutions were kept at 2×10^{-5} M, 8×10^{-5} M, and 4×10^{-5} M (i.e., 1:4:2). Fluorescence spectra of these solutions were recorded by excitation at 370 nm. Figure 10 shows the change in the fluorescence intensity of $[H_4L](ClO_4)_2$−metal perchlorate−Et_3N solutions for various metal ions. It can be seen clearly from Figure 10 that although Cd^{II} and Hg^{II} enhance the intensity moderately and slightly, respectively, Zn^{II} ion can turn on the fluorescence intensity significantly. The ratio of

dx.doi.org/10.1021/ic300412u | Inorg. Chem. 2012, 51, 8739−8749

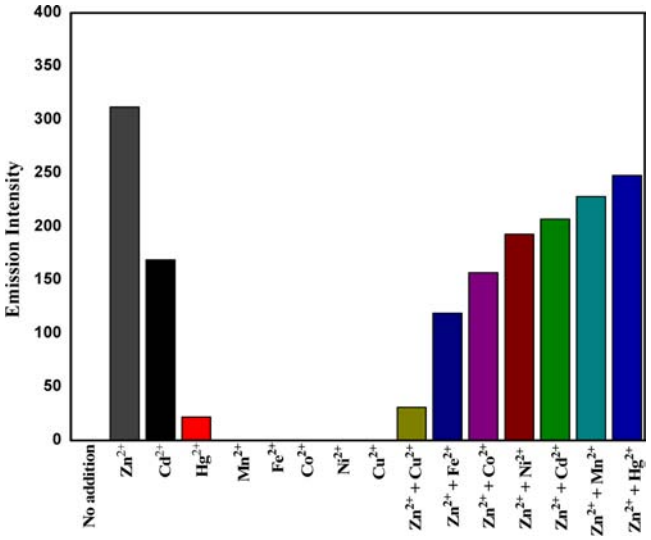

Figure 10. Fluorescence intensity profile of diprotonated macrocyclic salt $[H_4L](ClO_4)_2$ (2×10^{-5} M) in presence of various first-row transition metal ions (4×10^{-5} M) along with base (8×10^{-5} M) in acetonitrile at room temperature (excitation wavelength = 370 nm).

fluorescence intensity for Zn^{II}, Cd^{II}, and Hg^{II} is about 14:8:1. The enhancement of fluorescence was attributed to chelation enhance fluorescence (CHEF). In presence of first-row transition metal cations, Mn, Fe, Co, Ni, and Cu, the ligand shows no emission signal, that is, nonemissive in nature.

To further explore the selectivity of the ligand for Zn^{II}, we measured the fluorescence intensity of acetonitrile solutions of $[H_4L](ClO_4)_2$, Et_3N, and mixture of two perchlorate salts of zinc(II) and a second metal ion, Cu^{II}, Ni^{II}, Co^{II}, Fe^{II}, Mn^{II}, Cd^{II}, or Hg^{II} having concentration ratio 1:4:2:2. As evident from Figure 10, the emission intensity of Zn^{II}-bound macrocyclic ligand are perturbed (quenching of fluorescence) to a different extent in the presence of the second metal ions.

Comparison of the Emission Properties of $[H_4L](ClO_4)_2$ and 1−9 with Those of the Reported Related Systems. Spectrophotometric and spectrofluorimetric titrations of $[H_4L](ClO_4)_2$ with Et_3N, zinc(II) acetate and cadmium(II) acetate are described above. Similar spectrophotometric and spectrofluorimetric titrations of similar two other macrocycles[15a,b] with Et_3N and zinc(II) acetate were reported previously, revealing similar results. Fluorescence spectra of few dizinc(II) complexes derived from two Robson type ligands were also reported previously. In all those previous reports, as in the compounds **1**−**8**, zinc(II) assisted fluorescence enhancement takes place. However, no fluorescence spectra of cadmium(II) complexes derived from related macrocycles have been reported.

For some organic fluorophores for which Zn^{II} assisted enhancement takes place, enhancement/quenching by one or more of the metal ions among Cd^{II}, Hg^{II}, Cu^{II}, Ni^{II}, Co^{II}, Fe^{II}, and Mn^{II} has also been studied.[10a,b,d,11a,b,d,12,16c,f,g] Cadmium(II) in these examples is known to enhance significantly in some cases including those in which Cd^{II} enhances more than Zn^{II}.[12a,g,i] On the other hand, there are examples in which ligand fluorescence is unchanged and even quenched by Cd^{II}.[10b,12j,k] In the case of mercury(II), ligand fluorescence becomes either slightly enhanced, slightly quenched, or unchanged.[10a,b,d,12b,h,g] In the cases of Cu^{II}, Ni^{II}, Co^{II}, Fe^{II}, and Mn^{II}, ligand fluorescence becomes either slightly enhanced or slightly quenched, or unchanged.[10a,b,d,11a,b,d,12a,b,e,g−k] Thus, on the basis of results obtained so far, it is not possible to predict the effect of other metal ions on the fluorescence of a ligand for which zinc(II)-assisted fluorescence enhancement takes place. However, although quenching studies of ligand fluorescence is not possible in our case, the significant enhancement by cadmium(II), slight enhancement by mercury(II), and no change (nonemissive) by Cu^{II}, Ni^{II}, Co^{II}, Fe^{II}, and Mn^{II} are in line with some of the previous studies.

For some organic fluorophores for which Zn^{II} assisted enhancement takes place, metal ion competition studies (competition of Zn^{II} with other metal ions such as $Cu^{II}/Ni^{II}/Co^{II}/Fe^{II}/Mn^{II}/Cd^{II}/Hg^{II}$) have also been reported.[10a,b,d,11a,b,d,12,16c,f,g] In these cases, the zinc(II) assisted fluorescence enhancement either remains unchanged or is quenched to a different extent. No effect of other metal ions indicates that zinc(II) is better coordinated with that ligand in comparison to the other metal ions. On the other hand, better coordination of a metal ion than zinc(II) is indicated by quenching. According to the Irving−Williams order of stability, the order of the extent of quenching of the Zn^{II}-assisted enhanced fluorescence should be $Cu^{II} > Ni^{II} > Co^{II} > Fe^{II} > Mn^{II}$. Such order, in fact, has been observed in some cases.[12a,g] Again, according to best stability of copper(II) complexes, 100% quenching of Zn^{II}-assisted enhanced fluorescence by Cu^{II} has also been observed.[10a,12a] Examples are known in which Cu^{II} quenches Zn^{II}-assisted enhanced fluorescence completely, while the metal ions $Ni^{II}/Fe^{II}/Mn^{II}$ have no effect.[12a] On the other hand, complete quenching by Cu^{II} and also by Ni^{II} and Co^{II} is also known,[12c] which is definitely not as per Irving−Williams order. There are other cases also in which the Zn^{II}-assisted enhanced fluorescence is quenched by all of $Cu^{II}/Ni^{II}/Co^{II}/Fe^{II}/Mn^{II}$ but not according to Irving−Williams order; the order being $Cu^{II} > Co^{II} > Ni^{II} > Fe^{II} > Mn^{II}$.[11f] Interesting examples of zinc(II) specific systems are also known in which other metal ions (Cu^{II} and Mn^{II} or Ni^{II}, Fe^{II} and Mn^{II}) have no effect on the Zn^{II}-assisted enhanced fluorescence.[12j,16f,g] Clearly, the reported results regarding the competition studies are of different types, and it is not possible to predict in priori but depends on the specific case. In the previously reported examples of Zn^{II} + Cd^{II} or Zn^{II} + Hg^{II} competitive studies, it is known that quenching of Zn^{II}-assisted enhanced fluorescence takes place. In the present investigation, competition of Zn^{II} with metal ions Cu^{II}, Ni^{II}, Co^{II}, Fe^{II}, Mn^{II}, and Cd^{II}, and also Hg^{II} has been studied. In all these cases, quenching of the Zn^{II}-assisted enhanced fluorescence takes place, the order being $Cu^{II} > Fe^{II} > Co^{II} > Ni^{II} > Cd^{II} > Mn^{II} > Hg^{II}$. As shown in Figure 10, complete quenching has not taken place even by Cu^{II}. For the bivalent transition metal ions, although Cu^{II} and Mn^{II} lie at the two extremes in the quenching order, quenching order does not follow the Irving−Williams order for Ni^{II}, Co^{II}, and Fe^{II}. It may be noted that the order of the extent of quenching of the Zn^{II}-assisted enhanced fluorescence by the bivalent metal ions in the present investigation does not match with any of the previous observations, again indicating the system specificity of the phenomena.

It is relevant to mention the possible factors responsible for quenching the Zn^{II}-assisted enhanced fluorescence. The quenching by the paramagnetic metal ions takes place possibly because of the preferential coordination of these metal ions in comparison to zinc(II) and also by electron or energy transfer between the metal cation and the fluorophore, known as the fluorescence quenching mechanism.[26] Although Cd^{II} may be

dx.doi.org/10.1021/ic300412u | Inorg. Chem. 2012, 51, 8739−8749

better coordinated than Zn^{II} to the ligand system in this investigation, Hg^{II} should not be. So, while both the preferential coordination of Cd^{II} (than Zn^{II}) and heavy atom[27] enhanced intersystem crossing/spin−orbit coupling may be the possible reason of quenching by Cd^{II}, only the latter factor is responsible for the quenching by Hg^{II}.

CONCLUSIONS

The role of coordination anions on the fluorescence behavior of zinc(II) systems, as described in this report, is a new observation. We have observed a relationship between the radiative rate constant and quantum yield for the dizinc(II) complexes: the more the value of K_r, the more the value of the quantum yield. The enhancement of the ligand fluorescence by zinc(II) and cadmium(II) has been well undertood from time-resolved studies in terms of the increase of the radiative rate constant. Metal ion competition studies indicate that quenching by different extents of the zinc(II)-assisted fluorescence enhancement takes place by all of the metal ions among Cd^{II}, Hg^{II}, Cu^{II}, Ni^{II}, Co^{II}, Fe^{II}, and Mn^{II}. The quenching order for the bivalent 3d metal ions, $Cu^{II} > Fe^{II} > Co^{II} > Ni^{II} > Mn^{II}$, is not matched with any of the previously reported similar studies using various types of organic ligands. The comparison of the metal ion competition studies with previous such reports reveal the system dependency of such properties, and thus it is not possible to frame a correlation, that is, to predict a priori the extent of enhancement/quenching in presence of zinc(II) and one more metal ion.

As significant fluorescence enhancement of $[H_4L](ClO_4)_2$ takes place in presence of zinc(II) and cadmium(II), this ligand system may be used to identify these two metal ions. In biosystem where there is no Cd^{II}, this ligand system may be used to detect chelatable zinc(II). As the excitation wavelength, 370 nm, is sufficiently longer, no cell damage is expected and so this ligand system may be useful as a fluorescence imaging probe of zinc(II) ions in biosystems.[9,11f,12k,i,16c,f,g] The dizinc(II) complexes **1**−**8** may also be checked to behave as cancer therapy agents,[28a] as catalysts for copolymerization of CO_2 and cyclohexene oxide,[28b] and also as the precursor for interesting structural motifs including molecular ladders.[15g]

ASSOCIATED CONTENT

Supporting Information

Crystallographic data of **1**−**9** in CIF format, Scheme S1 Figures S1−S30, and Tables S1−S10. This material is available free of charge via the Internet at http://pubs.acs.org.

AUTHOR INFORMATION

Corresponding Author

*E-mail: sm_cu_chem@yahoo.co.in (S. Mohanta), samitmaj@gmail.com (S. Majumder).

Notes

The authors declare no competing financial interest.

ACKNOWLEDGMENTS

Financial support from the Government of India through Department of Science and Technology (Project No. SR/S1/IC-42/2011), Council for Scientific and Industrial Research (Fellowships to S. Majumder), and University Grants Commission (Fellowship to L. Mandal) is gratefully acknowledged. DST-FIST is acknowledged for providing the Crystallographic and TCSPC systems at the Department of Chemistry, University of Calcutta.

REFERENCES

(1) Lippard, S. J.; Berg, J. M. *Principles of Bioinorganic Chemistry*; University Science Books: Mill Valley, CA, 1994.

(2) Vallee, B. L.; Falchuk, K. H. *Physiol. Rev.* **1993**, *73*, 79.

(3) Coleman, J. E. *Curr. Opin. Chem. Biol.* **1998**, *2*, 222.

(4) (a) Lipscomb, W. N.; Sträter, N. *Chem. Rev.* **1996**, *96*, 2375. (b) Wilcox, D. E. *Chem. Rev.* **1996**, *96*, 2435. (c) Sträter, N.; Lipscomb, W. N.; Klabunde, T.; Crebs, B. *Angew. Chem., Int. Ed. Engl.* **1996**, *35*, 2024. (d) Steinhagen, H.; Helmchem, G. *Angew. Chem., Int. Ed. Engl.* **1996**, *35*, 2339.

(5) (a) Dealwis, C. G.; Chen, L.; Brennan, C.; Mandecki, C.; AbadZaptero, C. *Protein Eng.* **1995**, *8*, 865. (b) Zhang, Y.; Liang, J. Y.; Huang, H.; Ke, H.; Lipscomb, W. N. *Biochemistry* **1993**, *32*, 7844. (c) Burley, S. K.; David, P. R.; Taylor, A.; Lipscomb, W. N. *Proc. Natl. Acad. Sci. U.S.A.* **1990**, *87*, 6878.

(6) (a) Dia, Z.; Canary, J. W. *New J. Chem.* **2007**, 1708. (b) Liang, J.; Zhang, J.; Zhu, L.; Duarandin, A.; Young, V. G., Jr.; Geacintov, N.; Canary, J. W. *Inorg. Chem.* **2009**, *48*, 11196. (c) Royzen, M.; Durandin, A.; Young, V. G., Jr.; Geacintov, N. E.; Canary, J. W. *J. Am. Chem. Soc.* **2006**, *128*, 3854.

(7) (a) Ghosh, P.; Bharadwaj, P. K.; Mandal, S.; Ghosh, S. *J. Am. Chem. Soc.* **1996**, *118*, 1553. (b) Ahamed, B. N.; Ghosh, P. *Inorg. Chim. Acta* **2011**, *372*, 100. (c) Ahamed, B. N.; Ghosh, P. *J. Chem. Soc., Dalton Trans.* **2011**, 12540.

(8) (a) Patra, S.; Boricha, V. P.; Sreenidhi, K. R.; Suresh, E.; Paul, P. *Inorg. Chim. Acta* **2010**, *363*, 1639. (b) Maity, D.; Chakraborty, A.; Gunupuru, R.; Paul, P. *Inorg. Chim. Acta* **2011**, *372*, 126. (c) Fry, N. L.; Wei, J.; Mascharak, P. K. *Inorg. Chem.* **2011**, *50*, 9045.

(9) Jiang, P.; Guo, Z. *Coord. Chem. Rev.* **2004**, *248*, 205 , and references therein.

(10) (a) Hung, C.-H.; Chang, G.-F.; Kumar, A.; Lin, G.-F.; Luo, L.-Y.; Ching, W. -M.; Diau, E. W.-G. *Chem. Commun.* **2008**, 978. (b) Zhu, J.-F.; Yuan, H.; Chan, W.-H.; Lee, A. W. M. *Org. Biomol. Chem.* **2010**, 3957. (c) Buncic, G.; Donnelly, P. S.; Paterson, B. M.; White, J. M.; Zimmermann, M.; Xiao, Z.; Wedd, A. G. *Inorg. Chem.* **2010**, *49*, 3071. (d) Chen, H.; Wu, Y.; Cheng, Y.; Yang, H.; Li, F.; Yang, P.; Huang, C. *Inorg. Chem. Commun.* **2007**, *10*, 1413. (e) Mizukami, S.; Okada, S.; Kimura, S.; Kikuchi, K. *Inorg. Chem.* **2009**, *48*, 7630. (f) Kikuchi, K.; Komatsu, K.; Nagano, T. *Curr. Opin. Chem. Biol.* **2004**, *8*, 182. (g) Kimura, E.; Aoki, S. *BioMetals* **2001**, *14*, 191.

(11) (a) Komatsu, K.; Kikuchi, K.; Kojima, H.; Urano, Y.; Nagano, T. *J. Am. Chem. Soc.* **2005**, *127*, 10197. (b) Hirano, T.; Kikuchi, K.; Urano, Y.; Nagano, T. *J. Am. Chem. Soc.* **2002**, *124*, 6555. (c) Hirano, T.; Kikuchi, K.; Urano, Y.; Higuchi, T.; Nagano, T. *J. Am. Chem. Soc.* **2000**, *122*, 12399. (d) Maruyama, S.; Kikuchi, K.; Hirano, T.; Urano, Y.; Nagano, T. *J. Am. Chem. Soc.* **2002**, *124*, 10650. (e) Hirano, T.; Kikuchi, K.; Urano, Y.; Higuchi, T.; Nagano, T. *Angew. Chem., Int. Ed.* **2000**, *39*, 1052. (f) Hanaka, K.; Kikuchi, K.; Kojima, H.; Urano, Y.; Nagano, T. *J. Am. Chem. Soc.* **2004**, *126*, 12470.

(12) (a) Mikata, Y.; Wakamatsu, M.; Kawamura, A.; Yamanaka, N.; Yano, S.; Odani, A.; Morihiro, K.; Tamotsu, S. *Inorg. Chem.* **2006**, *45*, 9262. (b) Zhang, X.-a.; Lovejoy, K. S.; Jasanoff, A.; Lippard, S. J. *Proc. Natl. Acad. Sci.* **2007**, *104*, 10780. (c) Hung, C.-H.; Chang, G.-F.; Kumar, A.; Lin, G.-F.; Luo, L.-Y.; Ching, W.-M.; Diau, E. W.-G. *Chem. Commun.* **2008**, 978. (d) Liu, Z-c.; Wang, B-d.; Yang, Z-y.; Li, T-r.; Li, Y. *Inorg. Chem. Commun.* **2010**, *13*, 606. (e) Zhu, J.-F.; Yuan, H.; Chan, W.-H.; Lee, A. W. M. *Org. Biomol. Chem.* **2010**, *8*, 3957. (f) Mikata, Y.; Yamanaka, A.; Yamashita, A.; Yano, S. *Inorg. Chem.* **2008**, *47*, 7295. (g) Sarkar, A.; Ghosh, A. K.; Bertolasi, V.; Ray, D. *Dalton Trans.* **2012**, *41*, 1889. (h) Peng, X.; Tang, X.; Qin, W.; Dou, W.; Gou, Y.; Zheng, J.; Liu, W.; Wang, D. *Dalton Trans.* **2011**, *40*, 5271. (i) Wu, Y.; Peng, X.; Guo, B.; Fan, J.; Zhang, Z.; Wang, J.; Cui, A.; Gao, Y. *Org. Biomol. Chem.* **2005**, *3*, 1387. (j) Saha, U. C.; Chattopadhyay, B.; Dhara, K.; Mandal, S. K.; Sarkar, S.; Khuda-Bukhsh, A. R.; Mukherjee, M.; Helliwell, M.; Chattopadhyay, P. *Inorg.*

Chem. **2011**, *50*, 1213. (k) Sasaki, H.; Hanaoka, K.; Urano, Y.; Terai, T.; Nagano, T. *Biorg. Med. Chem.* **2011**, *19*, 1072.
(13) (a) Liu, W.; Xu, L.; Sheng, R.; Wang, P.; Li, H.; Wu, S. *Org. Lett.* **2007**, *9*, 3829. (b) Tang, X.-L.; Peng, X.-H.; Dou, W.; Mao, J.; Zheng, J.-R.; Qin, W.-W.; Liu, W.-S.; Chang, J.; Yao, X.-J. *Org. Lett.* **2008**, *10*, 3653. (c) Xue, L.; Liu, Q.; Jiang, H. *Org. Lett.* **2009**, *11*, 3454.
(14) (a) Thompson, L. K.; Mandal, S. K.; Tandon, S. S.; Bridson, J. N.; Park, M. K. *Inorg. Chem.* **1996**, *35*, 3117. (b) Hazra, S.; Majumder, S.; Fleck, M.; Aliage-Alcalde, N.; Mohanta, S. *Polyhedron* **2009**, *28*, 3707. (c) Gou, S.; Qian, M.; Yu, Z.; Duan, C.; Sun, X.; Huang, W. *J. Chem. Soc., Dalton Trans.* **2001**, 3232. (d) Liu, B.; Zhou, H.; Pan, Z.; Zhang, H.; Hu, J.; Hu, X.; Zhou, H.; Song, Y. *Trans. Met. Chem.* **2005**, *30*, 1020. (e) Lacroix, P.; Kahn, O.; Theobald, F.; Leroy, J.; Wakselman, C. *Inorg. Chim. Acta* **1988**, *142*, 129.
(15) (a) Dutta, B.; Bag, P.; Flörke, U.; Nag, K. *Inorg. Chem.* **2005**, *44*, 147. (b) Hazra, S.; Majumder, S.; Fleck, M.; Koner, R.; Mohanta, S. *Polyhedron* **2009**, *28*, 2871. (c) Atkins, A. J.; Black, D.; Finn, R. L.; Marin-Becerra, A.; Blake, A. J.; Ruiz-Ramirez, L.; Li, W.-S.; Schröder, M. *J. Chem. Soc., Dalton Trans.* **2003**, 1730. (d) Adams, H.; Bailey, N. A.; Bertrand, P.; Rodriguez de Barbarin, C. O.; Fenton, D. E.; Gou, S. *J. Chem. Soc., Dalton Trans.* **1995**, 275. (e) Huang, W.; Gou, S.; Hu, D.; Chantrapromma, S.; Fun, H.-K.; Meng, Q. *Inorg. Chem.* **2002**, *41*, 864. (f) Ponsico, S.; Gulyas, H.; Marta-Belmonte, M.; Escudero-Adán, E. C.; Freixa, Z.; van Leeuwen, P. W. N. M. *Dalton Trans.* **2011**, 10686. (g) Huang, W.; Zhu, H.-B.; Gou, S.-H. *Coord. Chem. Rev.* **2006**, *250*, 414.
(16) (a) Hosseini-Yazdi, S. A.; Khandar, A. A.; Tabatabai, M. K.; Noohinejad, L. *Z. Anorg. Allg. Chem.* **2010**, *636*, 2650. (b) Seward, C.; Pang, J.; Wang, S. *Eur. J. Inorg. Chem.* **2002**, 1390. (c) Roy, P.; Dhara, K.; Manassero, M.; Ratha, J.; Banerjee, P. *Inorg. Chem.* **2007**, *46*, 6405. (d) Roy, P.; Manassero, M.; Dhara, K.; Banerjee, P. *Polyhedron* **2009**, *28*, 1133. (e) Majumder, A.; Rosair, G. M.; Mallick, A.; Chattopadhyay, N.; Mitra, S. *Polyhedron* **2006**, *25*, 1753. (f) Sarkar, K.; Dhara, K.; Nandi, M.; Roy, P.; Bhaumik, A.; Banerjee, P. *Adv. Funct. Mater.* **2009**, *19*, 223. (g) Dhara, K.; Karan, S.; Ratha, J.; Roy, P.; Chandra, G.; Manassero, M.; Mallik, B.; Banerjee, P. *Chem.—Asian J.* **2007**, *2*, 1091. (h) Yu, T.; Zhang, K.; Zhao, Y.; Yang, C.; Zhang, H.; Qian, L.; Fan, D.; Dong, W.; Chen, L.; Qiu, Y. *Inorg. Chim. Acta* **2008**, *361*, 233. (i) Chen, J.-Q.; Cai, Y.-P.; Fang, H.-C.; Zhou, Z.-Y.; Zhan, X.-L.; Zhao, G.; Zhang, Z. *Crys. Growth Des.* **2009**, *9*, 1605. (j) Yu, T.; Zhang, K.; Zhao, Y.; Yang, C.; Zhang, H.; Fan, D.; Dong, W. *Inorg. Chem. Commun.* **2007**, *10*, 401.
(17) (a) Fang, H.-C.; Zhu, J.-Q.; Zhou, L.-J.; Jia, H.-Y.; Li, S.-S.; Gong, X.; Li, S.-B.; Cai, Y.-P.; Thallapally, P. K.; Liu, J.; Exarhos, G. J. *Cryst. Growth Des.* **2010**, *10*, 3277. (b) Fang, H.-C.; Yi, X.-Y.; Gu, Z.-G.; Zhao, G.; Wen, Q.-Y.; Zhu, J.-Q.; Xu, A.-W.; Cai, Y.-P. *Cryst. Growth Des.* **2009**, *9*, 3776. (c) Lo, W.-K.; Wong, W.-K.; Wong, W.-Y.; Guo, J. *Eur. J. Inorg. Chem.* **2005**, 3950. (d) Zhou, X.-X.; Cai, Y.-P.; Zhu, S.-Z.; Zhan, Q.-G.; Liu, M.-S.; Zhou, Z.-Y.; Chen, L. *Cryst. Growth Des.* **2008**, *8*, 2076. (e) Roy, P. *J. Coord. Chem.* **2009**, *62*, 2003. (f) Chakraborty, J.; Thakurta, S.; Samanta, B.; Ray, A.; Pilet, G.; Batten, S. R.; Jensen, P.; Mitra, S. *Polyhedron* **2007**, *26*, 5139.
(18) (a) Majumder, S.; Sarkar, S.; Sasmal, S.; Sañudo, E. C.; Mohanta, S. *Inorg. Chem.* **2011**, *50*, 7540. (b) Majumder, S.; Fleck, M.; Lucas, C. R.; Mohanta, S. *J. Mol. Struct.* **2012**, *1020*, 127.
(19) Ullman, F.; Brittner, K. *Chem. Ber.* **1909**, *42*, 2539.
(20) (a) Dawson, W. R.; Windsor, M. W. *J. Phys. Chem.* **1968**, *72*, 3251. (b) Melhuish, W. H. *J. Phys. Chem.* **1961**, *65*, 229. (c) Parker, C. A.; Rees, W. T. *Analyst* **1960**, *85*, 587. (d) Paul, B. K.; Guchhait, N. *J. Phys. Chem. B* **2010**, *114*, 12528. (e) Paul, B. K.; Guchhait, N. *J. Phys. Chem. B* **2011**, *115*, 11938. (f) Paul, B. K.; Guchhait, N. *J. Phys. Chem. B* **2011**, *115*, 10322. (g) Suresh, M.; Jose, D. A.; Das, A. *Org. Lett.* **2007**, *9*, 441. (h) Ahmad, I.; Fasihullah, Q.; Vaid, F. H. M. *J. Photochem. Photobiol. B* **2005**, *78*, 229.
(21) (a) Lakowicz, J. R. *Priniples of Fluorescence Spectroscopy*, 3rd ed.; Plenum: New York, 2006. (b) Paul., B. K.; Guchhait, N. *J. Phys. Chem. B* **2011**, *115*, 10322.
(22) (a) *APEX-II, SAINT-Plus and TWINABS*; Bruker-Nonius AXS Inc.: Madison, WI, 2004. (b) Sheldrick, G. M. *SAINT (Version 6.02), SADABS (Version 2.03)*; Bruker AXS lnc.: Madison, WI, 2002. (c) *SHELXTL*, version 6.10; Bruker AXS Inc.: Madison, WI, 2002. (d) Sheldrick, G. M. *SHELXL-97, Crystal Structure Refinement Program*; University of Göttingen: Göttingen, Germany, 1997.
(23) Geary, W. J. *Chem. Rev.* **1971**, *7*, 81.
(24) Dutta, B.; Bag, P.; Adhikary, B.; Flörke, U.; Nag, K. *J. Org. Chem.* **2004**, *69*, 5419.
(25) Saitoh, M.; Balch, A. L.; Yuasa, J.; Kawai, T. *Inorg. Chem.* **2010**, *49*, 7129.
(26) Sarkar, M.; Banthia, S.; Samanta, A. *Tetrahedron Lett.* **2006**, *47*, 7575.
(27) (a) Rurack, K. *Spectrochim. Acta, Part A* **2001**, *57*, 2161. (b) Ahamed, B. N.; Ghosh, P. *J. Chem. Soc., Dalton Trans.* **2011**, 6411. (c) Suresh, M.; Das, A. *Tetrahedron Lett.* **2009**, *50*, 5808.
(28) (a) Gao, J.; Liu, Y.-G.; Zhou, Y.; Boxer, L. M.; Woolley, F. R.; Zingaro, R. A. *ChemBioChem* **2007**, *8*, 332. (b) Kember, M. R.; White, A. J. P.; Williams, C. K. *Inorg. Chem.* **2009**, *48*, 9535.